Unit – 4

IIR and FIR filters

The transfer function is obtained by taking Z transform of finite sample impulse response. The filters designed by using finite samples of impulse response are called FIR filters. Some of the advantages of FIR filter are linear phase, both recursive and non recursive, stable and round off noise can be made smaller.

Some of the disadvantages of FIR filters are large amount of processing is required and non integral delay may lead to problems.

DESIGN OF FIR FILTERS

An FIR filter of length M with input $x(n)$ and output $y(n)$ is described by the difference equation

$$y(n) = b_0x(n) + b_1x(n-1) + \cdots + b_{M-1}x(n-M+1)$$
$$= \sum_{k=0}^{M-1} b_k x(n-k) \qquad (8.2.1)$$

where $\{b_k\}$ is the set of filter coefficients. Alternatively, we can express the output sequence as the convolution of the unit sample response $h(n)$ of the system with the input signal. Thus we have

$$y(n) = \sum_{k=0}^{M-1} h(k)x(n-k) \qquad (8.2.2)$$

where the lower and upper limits on the convolution sum reflect the causality and finite-duration characteristics of the filter. Clearly, (8.2.1) and (8.2.2) are identical in form and hence it follows that $b_k = h(k)$, $k = 0, 1, \ldots, M-1$.

The filter can also be characterized by its system function

$$H(z) = \sum_{k=0}^{M-1} h(k)z^{-k} \qquad (8.2.3)$$

which we view as a polynomial of degree $M-1$ in the variable z^{-1}. The roots of this polynomial constitute the zeros of the filter.

An FIR filter has linear phase if its unit sample response satisfies the condition

$$h(n) = \pm h(M-1-n) \qquad n = 0, 1, \ldots, M-1 \qquad (8.2.4)$$

When the symmetry and antisymmetry conditions in (8.2.4) are incorporated into (8.2.3), we have

$$H(z) = h(0) + h(1)z^{-1} + h(2)z^{-2} + \cdots + h(M-2)z^{-(M-2)} + h(M-1)z^{-(M-1)}$$
$$= z^{-(M-1)/2}\left\{h\left(\frac{M-1}{2}\right) + \sum_{n=0}^{(M-3)/2} h(n)\left[z^{(M-1-2k)/2} \pm z^{-(M-1-2k)/2}\right]\right\} \quad M \text{ odd}$$
$$= z^{-(M-1)/2}\sum_{n=0}^{(M/2)-1} h(n)[z^{(M-1-2k)/2} \pm z^{-(M-1-2k)/2}] \qquad M \text{ even} \qquad (8.2.5)$$

Now, if we substitute z^{-1} for z in (8.2.3) and multiply both sides of the resulting equation by $z^{-(M-1)}$, we obtain

$$z^{-(M-1)}H(z^{-1}) = \pm H(z) \qquad (8.2.6)$$

When $h(n) = h(M-1-n)$, $H(\omega)$ can be expressed as

$$H(\omega) = H_r(\omega)e^{-j\omega(M-1)/2} \tag{8.2.7}$$

where $H_r(\omega)$ is a real function of ω and can be expressed as

$$H_r(\omega) = h\left(\frac{M-1}{2}\right) + 2\sum_{n=0}^{(M-3)/2} h(n)\cos\omega\left(\frac{M-1}{2} - n\right) \qquad M \text{ odd} \tag{8.2.8}$$

$$H_r(\omega) = 2\sum_{n=0}^{(M/2)-1} h(n)\cos\omega\left(\frac{M-1}{2} - n\right) \qquad M \text{ even} \tag{8.2.9}$$

The phase characteristic of the filter for both M odd and M even is

$$\Theta(\omega) = \begin{cases} -\omega\left(\dfrac{M-1}{2}\right), & \text{if } H_r(\omega) > 0 \\ -\omega\left(\dfrac{M-1}{2}\right) + \pi, & \text{if } H_r(\omega) < 0 \end{cases} \tag{8.2.10}$$

When

$$h(n) = -h(M-1-n)$$

the unit sample response is *antisymmetric*. For M odd, the center point of the antisymmetric $h(n)$ is $n = (M-1)/2$. Consequently,

$$h\left(\frac{M-1}{2}\right) = 0$$

It is straightforward to show that the frequency response of an FIR filter with an antisymmetric unit sample response can be expressed as

$$H(\omega) = H_r(\omega)e^{j[-\omega(M-1)/2+\pi/2]} \tag{8.2.11}$$

where

$$H_r(\omega) = 2\sum_{n=0}^{(M-3)/2} h(n)\sin\omega\left(\frac{M-1}{2} - n\right) \qquad M \text{ odd} \tag{8.2.12}$$

$$H_r(\omega) = 2\sum_{n=0}^{(M/2)-1} h(n)\sin\omega\left(\frac{M-1}{2} - n\right) \qquad M \text{ even} \tag{8.2.13}$$

The phase characteristic of the filter for both M odd and M even is

$$\Theta(\omega) = \begin{cases} \dfrac{\pi}{2} - \omega\left(\dfrac{M-1}{2}\right), & \text{if } H_r(\omega) > 0 \\ \dfrac{3\pi}{2} - \omega\left(\dfrac{M-1}{2}\right), & \text{if } H_r(\omega) < 0 \end{cases} \tag{8.2.14}$$

The choice of a symmetric or antisymmetric unit sample response depends on the application. As we shall see later, a symmetric unit sample response is suitable for some applications, while an antisymmetric unit sample response is more suitable for other applications. For example, if $h(n) = -h(M-1-n)$ and M is odd, (8.2.12) implies that $H_r(0) = 0$ and $H_r(\pi) = 0$. Consequently, (8.2.12) is not suitable as either a lowpass filter or a highpass filter. Similarly, the antisymmetric unit sample response with M even also results in $H_r(0) = 0$, as can be easily verified from (8.2.13). Consequently, we would not use the antisymmetric condition in the design of a lowpass linear-phase FIR filter. On the other hand, the symmetry condition $h(n) = h(M-1-n)$ yields a linear-phase FIR filter with a nonzero response at $\omega = 0$, if desired, that is,

$$H_r(0) = h\left(\frac{M-1}{2}\right) + 2\sum_{n=0}^{(M-3)/2} h(n), \qquad M \text{ odd} \tag{8.2.15}$$

$$H_r(0) = 2\sum_{n=0}^{(M/2)-1} h(n), \qquad M \text{ even} \tag{8.2.16}$$

8.2.2 Design of Linear-Phase FIR Filters Using Windows

In this method we begin with the desired frequency response specification $H_d(\omega)$ and determine the corresponding unit sample response $h_d(n)$. Indeed, $h_d(n)$ is related to $H_d(\omega)$ by the Fourier transform relation

$$H_d(\omega) = \sum_{n=0}^{\infty} h_d(n)e^{-j\omega n} \tag{8.2.17}$$

where

$$h_d(n) = \frac{1}{2\pi}\int_{-\pi}^{\pi} H_d(\omega)e^{j\omega n}d\omega \tag{8.2.18}$$

Thus, given $H_d(\omega)$, we can determine the unit sample response $h_d(n)$ by evaluating the integral in (8.2.18).

In general, the unit sample response $h_d(n)$ obtained from (8.2.17) is infinite in duration and must be truncated at some point, say at $n = M - 1$, to yield an FIR filter of length M. Truncation of $h_d(n)$ to a length $M - 1$ is equivalent to multiplying $h_d(n)$ by a "rectangular window," defined as

$$w(n) = \begin{cases} 1, & n = 0, 1, \ldots, M-1 \\ 0, & \text{otherwise} \end{cases} \tag{8.2.19}$$

Thus the unit sample response of the FIR filter becomes

$$\begin{aligned} h(n) &= h_d(n)w(n) \\ &= \begin{cases} h_d(n), & n = 0, 1, \ldots, M-1 \\ 0, & \text{otherwise} \end{cases} \end{aligned} \tag{8.2.20}$$

It is instructive to consider the effect of the window function on the desired frequency response $H_d(\omega)$. Recall that multiplication of the window function $w(n)$ with $h_d(n)$ is equivalent to convolution of $H_d(\omega)$ with $W(\omega)$, where $W(\omega)$ is the frequency-domain representation (Fourier transform) of the window function, that is,

$$W(\omega) = \sum_{n=0}^{M-1} w(n)e^{-j\omega n} \tag{8.2.21}$$

Thus the convolution of $H_d(\omega)$ with $W(\omega)$ yields the frequency response of the (truncated) FIR filter. That is,

$$H(\omega) = \frac{1}{2\pi}\int_{-\pi}^{\pi} H_d(\nu)W(\omega - \nu)d\nu \tag{8.2.22}$$

The Fourier transform of the rectangular window is

$$\begin{aligned} W(\omega) &= \sum_{n=0}^{M-1} e^{-j\omega n} \\ &= \frac{1 - e^{-j\omega M}}{1 - e^{-j\omega}} = e^{-j\omega(M-1)/2}\frac{\sin(\omega M/2)}{\sin(\omega/2)} \end{aligned} \tag{8.2.23}$$

This window function has a magnitude response

$$|W(\omega)| = \frac{|\sin(\omega M/2)|}{|\sin(\omega/2)|} \qquad -\pi \leq \omega \leq \pi \tag{8.2.24}$$

and a piecewise linear phase

$$\Theta(\omega) = \begin{cases} -\omega\left(\dfrac{M-1}{2}\right), & \text{when } \sin(\omega M/2) \geq 0 \\ -\omega\left(\dfrac{M-1}{2}\right) + \pi, & \text{when } \sin(\omega M/2) < 0 \end{cases} \tag{8.2.25}$$

The magnitude response of the window function is illustrated in Fig. 8.4 for $M = 31$ and 61. The width of the main lobe [width is measured to the first zero of $W(\omega)$]

Name of window	Time-domain sequence, $h(n),\ 0 \le n \le M-1$	
Bartlett (triangular)	$1 - \dfrac{2\left\lvert n - \dfrac{M-1}{2}\right\rvert}{M-1}$	
Blackman	$0.42 - 0.5\cos\dfrac{2\pi n}{M-1} + 0.08\cos\dfrac{4\pi n}{M-1}$	
Hamming	$0.54 - 0.46\cos\dfrac{2\pi n}{M-1}$	
Hanning	$\dfrac{1}{2}\left(1 - \cos\dfrac{2\pi n}{M-1}\right)$	
Kaiser	$\dfrac{I_0\left[\alpha\sqrt{\left(\dfrac{M-1}{2}\right)^2 - \left(n - \dfrac{M-1}{2}\right)^2}\right]}{I_0\left[\alpha\left(\dfrac{M-1}{2}\right)\right]}$	
Lanczos	$\left\{\dfrac{\sin\left[2\pi\left(n - \dfrac{M-1}{2}\right)\Big/(M-1)\right]}{2\pi\left(n - \dfrac{M-1}{2}\right)\Big/\left(\dfrac{M-1}{2}\right)}\right\}^L$	$L > 0$
Tukey	$1,\ \left\lvert n - \dfrac{M-1}{2}\right\rvert \le \alpha\dfrac{M-1}{2}$	$0 < \alpha < 1$
	$\dfrac{1}{2}\left[1 + \cos\left(\dfrac{n-(1+\alpha)(M-1)/2}{(1-\alpha)(M-1)/2}\pi\right)\right]$	
	$\alpha(M-1)/2 \le \left\lvert n - \dfrac{M-1}{2}\right\rvert \le \dfrac{M-1}{2}$	

8.2.3 Design of Linear-Phase FIR Filters by the Frequency-Sampling Method

In the frequency sampling method for FIR filter design, we specify the desired frequency response $H_d(\omega)$ at a set of equally spaced frequencies, namely

$$\begin{aligned}
\omega_k = \tfrac{2\pi}{M}(k+\alpha) \qquad & k = 0, 1, \ldots, \frac{M-1}{2} \quad M \text{ odd} \\
& k = 0, 1, \ldots, \frac{M}{2} - 1 \quad M \text{ even} \\
& \alpha = 0 \quad \text{or} \quad \tfrac{1}{2}
\end{aligned} \tag{8.2.30}$$

and solve for the unit sample response $h(n)$ of the FIR filter from these equally spaced frequency specifications. To reduce sidelobes, it is desirable to optimize the frequency specification in the transition band of the filter. This optimization can be accomplished numerically on a digital computer by means of linear programming techniques as shown by Rabiner et al. (1970).

In this section we exploit a basic symmetry property of the sampled frequency response function to simplify the computations. Let us begin with the desired frequency response of the FIR filter, which is [for simplicity, we drop the subscript in $H_d(\omega)$],

$$H(\omega) = \sum_{n=0}^{M-1} h(n)e^{-j\omega n} \tag{8.2.31}$$

Suppose that we specify the frequency response of the filter at the frequencies given by (8.2.30). Then from (8.2.31) we obtain

$$H(k+\alpha) \equiv H\left(\frac{2\pi}{M}(k+\alpha)\right)$$

$$H(k+\alpha) \equiv \sum_{n=0}^{M-1} h(n)e^{-j2\pi(k+\alpha)n/M} \qquad k = 0, 1, \ldots, M-1 \tag{8.2.32}$$

It is a simple matter to invert (8.2.32) and express $h(n)$ in terms of $H(k+\alpha)$. If we multiply both sides of (8.2.32) by the exponential, $\exp(j2\pi km/M)$, $m = 0, 1, \ldots, M-1$, and sum over $k = 0, 1, \ldots, M-1$, the right-hand side of (8.2.32) reduces to $Mh(m)\exp(-j2\pi\alpha m/M)$. Thus we obtain

$$h(n) = \frac{1}{M}\sum_{k=0}^{M-1} H(k+\alpha)e^{j2\pi(k+\alpha)n/M} \qquad n = 0, 1, \ldots, M-1 \tag{8.2.33}$$

The relationship in (8.2.33) allows us to compute the values of the unit sample response $h(n)$ from the specification of the frequency samples $H(k+\alpha)$, $k = 0, 1, \ldots, M-1$. Note that when $\alpha = 0$, (8.2.32) reduces to the discrete Fourier transform (DFT) of the sequence $\{h(n)\}$ and (8.2.33) reduces to the inverse DFT (IDFT).

Since $\{h(n)\}$ is real, we can easily show that the frequency samples $\{H(k+\alpha)\}$ satisfy the symmetry condition

$$H(k+\alpha) = H^*(M-k-\alpha) \tag{8.2.34}$$

This symmetry condition, along with the symmetry conditions for $\{h(n)\}$, can be used to reduce the frequency specifications from M points to $(M+1)/2$ points for M odd and $M/2$ points for M even. Thus the linear equations for determining $\{h(n)\}$ from $\{H(k+\alpha)\}$ are considerably simplified.

In particular, if (8.2.11) is sampled at the frequencies $\omega_k = 2\pi(k+\alpha)/M$, $k = 0, 1, \ldots, M-1$, we obtain

$$H(k+\alpha) = H_r\left(\frac{2\pi}{M}(k+\alpha)\right)e^{j[\beta\pi/2-2\pi(k+\alpha)(M-1)/2M]} \tag{8.2.35}$$

where $\beta = 0$ when $\{h(n)\}$ is symmetric and $\beta = 1$ when $\{h(n)\}$ is antisymmetric. A simplication occurs by defining a set of real frequency samples $\{G(k+m)\}$

$$G(k+\alpha) = (-1)^k H_r\left(\frac{2\pi}{M}(k+\alpha)\right) \qquad k = 0, 1, \ldots, M-1 \tag{8.2.36}$$

We use (8.2.36) in (8.2.35) to eliminate $H_r(\omega_k)$. Thus we obtain

$$H(k+\alpha) = G(k+\alpha)e^{j\pi k}e^{j[\beta\pi/2 - 2\pi(k+\alpha)(M-1)/2M]} \tag{8.2.37}$$

Now the symmetry condition for $H(k+\alpha)$ given in (8.2.34) translates into a corresponding symmetry condition for $G(k+\alpha)$, which can be exploited by substituting into (8.2.33), to simplify the expressions for the FIR filter impulse response $\{h(n)\}$ for the four cases $\alpha = 0$, $\alpha = \frac{1}{2}$, $\beta = 0$, and $\beta = 1$. The results are summarized in Table 8.3. The detailed derivations are left as exercises for the reader.

8.2.4 Design of Optimum Equiripple Linear-Phase FIR Filters

The window method and the frequency-sampling method are relatively simple techniques for designing linear-phase FIR filters. However, they also possess some minor disadvantages, described in Section 8.2.6, which may render them undesirable for some applications. A major problem is the lack of precise control of the critical frequencies such as ω_p and ω_s.

The filter design method described in this section is formulated as a Chebyshev approximation problem. It is viewed as an optimum design criterion in the sense that the weighted approximation error between the desired frequency response and the actual frequency response is spread evenly across the passband and evenly across the stopband of the filter minimizing the maximum error. The resulting filter designs have ripples in both the passband and the stopband.

To describe the design procedure, let us consider the design of a lowpass filter with passband edge frequency ω_p and stopband edge frequency ω_s. From the general specifications given in Fig. 8.2, in the passband, the filter frequency response satisfies the condition

$$1 - \delta_1 \le H_r(\omega) \le 1 + \delta_1 \qquad |\omega| \le \omega_p \tag{8.2.43}$$

Similarly, in the stopband, the filter frequency response is specified to fall between the limits $\pm\delta_2$, that is,

$$-\delta_2 \le H_r(\omega) \le \delta_2 \qquad |\omega| > \omega_s \tag{8.2.44}$$

Thus δ_1 represents the ripple in the passband and δ_2 represents the attenuation or ripple in the stopband. The remaining filter parameter is M, the filter length or the number of filter coefficients.

Case 1: Symmetric unit sample response $h(n) = h(M-1-n)$ and M Odd. In this case, the real-valued frequency response characteristic $H_r(\omega)$ is

$$H_r(\omega) = h\left(\frac{M-1}{2}\right) + 2\sum_{n=0}^{(M-3)/2} h(n)\cos\omega\left(\frac{M-1}{2} - n\right) \tag{8.2.45}$$

If we let $k = (M-1)/2 - n$ and define a new set of filter parameters $\{a(k)\}$ as

$$a(k) = \begin{cases} h\left(\dfrac{M-1}{2}\right), & k = 0 \\ 2h\left(\dfrac{M-1}{2} - k\right), & k = 1, 2, \ldots, \dfrac{M-1}{2} \end{cases} \tag{8.2.46}$$

then (8.2.45) reduces to the compact form

$$H_r(\omega) = \sum_{k=0}^{(M-1)/2} a(k)\cos\omega k \tag{8.2.47}$$

Case 2: Symmetric unit sample response $h(n) = h(M-1-n)$ and M Even. In this case, $H_r(\omega)$ is expressed as

$$H_r(\omega) = 2\sum_{n=0}^{(M/2)-1} h(n)\cos\omega\left(\frac{M-1}{2} - n\right) \tag{8.2.48}$$

Again, we change the summation index from n to $k = M/2 - n$ and define a new set of filter parameters $\{b(k)\}$ as

$$b(k) = 2h\left(\frac{M}{2} - k\right), k = 1, 2, \ldots, M/2 \tag{8.2.49}$$

With these substitutions (8.2.48) becomes

$$H_r(\omega) = \sum_{k=1}^{M/2} b(k)\cos\omega\left(k - \frac{1}{2}\right) \tag{8.2.50}$$

In carrying out the optimization, it is convenient to rearrange (8.2.50) further into the form

$$H_r(\omega) = \cos\frac{\omega}{2}\sum_{k=0}^{(M/2)-1} \tilde{b}(k)\cos\omega k \tag{8.2.51}$$

where the coefficients $\{\tilde{b}(k)\}$ are linearly related to the coefficients $\{b(k)\}$. In fact, it can be shown that the relationship is

$$\begin{aligned} \tilde{b}(0) &= \tfrac{1}{2}b(1) \\ \tilde{b}(k) &= 2b(k) - \tilde{b}(k-1) \qquad k = 1, 2, 3, \ldots, \frac{M}{2} - 2 \\ \tilde{b}\left(\frac{M}{2} - 1\right) &= 2b\left(\frac{M}{2}\right) \end{aligned} \tag{8.2.52}$$

Case 3: Antisymmetric unit sample response $h(n) = -h(M-1-n)$ and M Odd. The real-valued frequency response characteristic $H_r(\omega)$ for this case is

$$H_r(\omega) = 2 \sum_{n=0}^{(M-3)/2} h(n) \sin \omega \left(\frac{M-1}{2} - n \right) \tag{8.2.53}$$

If we change the summation in (8.2.53) from n to $k = (M-1)/2 - n$ and define a new set of filter parameters $\{c(k)\}$ as

$$c(k) = 2h\left(\frac{M-1}{2} - k\right) \qquad k = 1, 2, \ldots, (M-1)/2 \tag{8.2.54}$$

then (8.2.53) becomes

$$H_r(\omega) = \sum_{k=1}^{(M-1)/2} c(k) \sin \omega k \tag{8.2.55}$$

As in the previous case, it is convenient to rearrange (8.2.55) into the form

$$H_r(\omega) = \sin \omega \sum_{k=0}^{(M-3)/2} \tilde{c}(k) \cos \omega k \tag{8.2.56}$$

Case 4: Antisymmetric unit sample response $h(n) = -h(M-1-n)$ and M Even. In this case, the real-valued frequency response characteristic $H_r(\omega)$ is

$$H_r(\omega) = 2 \sum_{n=0}^{(M/2)-1} h(n) \sin \omega \left(\frac{M-1}{2} - n \right) \tag{8.2.58}$$

A change in the summation index from n to $k = M/2 - n$ combined with a definition of a new set of filter coefficients $\{d(k)\}$, related to $\{h(n)\}$ according to

$$d(k) = 2h\left(\frac{M}{2} - k\right) \qquad k = 1, 2, \ldots, \frac{M}{2} \tag{8.2.59}$$

results in the expression

$$H_r(\omega) = \sum_{k=1}^{M/2} d(k) \sin \omega \left(k - \frac{1}{2} \right) \tag{8.2.60}$$

As in the previous two cases, we find it convenient to rearrange (8.2.60) into the form

$$H_r(\omega) = \sin \frac{\omega}{2} \sum_{k=0}^{(M/2)-1} \tilde{d}(k) \cos \omega k \tag{8.2.61}$$

Filter type	$Q(\omega)$	$P(\omega)$
$h(n) = h(M-1-n)$ M odd (case 1)	1	$\sum_{k=0}^{(M-1)/2} a(k) \cos \omega k$
$h(n) = h(M-1-n)$ M even (case 2)	$\cos \frac{\omega}{2}$	$\sum_{k=0}^{(M/2)-1} \tilde{b}(k) \cos \omega k$
$h(n) = -h(M-1-n)$ M odd (case 3)	$\sin \omega$	$\sum_{k=0}^{(M-3)/2} \tilde{c}(k) \cos \omega k$
$h(n) = -h(M-1-n)$ M even (case 4)	$\sin \frac{\omega}{2}$	$\sum_{k=0}^{(M/2)-1} \tilde{d}(k) \cos \omega k$

IIR FILTER DESIGN

DESIGN OF IIR FILTERS FROM ANALOG FILTERS

Just as in the design of FIR filters, there are several methods that can be used to design digital filters having an infinite-duration unit sample response. The techniques described in this section are all based on converting an analog filter into a digital filter. Analog filter design is a mature and well developed field, so it is not surprising that we begin the design of a digital filter in the analog domain and then convert the design into the digital domain.

An analog filter can be described by its system function.

$$H_a(s) = \frac{B(s)}{A(s)} = \frac{\sum_{k=0}^{M} \beta_k s^k}{\sum_{k=0}^{N} \alpha_k s^k} \tag{8.3.1}$$

where $\{\alpha_k\}$ and $\{\beta_k\}$ are the filter coefficients, or by its impulse response, which is related to $H_a(s)$ by the Laplace transform

$$H_a(s) = \int_{-\infty}^{\infty} h(t)e^{-st}\,dt \tag{8.3.2}$$

Alternatively, the analog filter having the rational system function $H(s)$ given in (8.3.1), can be described by the linear constant-coefficient differential equation

$$\sum_{k=0}^{N} \alpha_k \frac{d^k y(t)}{dt^k} = \sum_{k=0}^{M} \beta_k \frac{d^k x(t)}{dt^k} \tag{8.3.3}$$

where $x(t)$ denotes the input signal and $y(t)$ denotes the output of the filter.

Each of these three equivalent characterizations of an analog filter leads to alternative methods for converting the filter into the digital domain, as will be described in Sections 8.3.1 through 8.3.4. We recall that an analog linear time-invariant system with system function $H(s)$ is stable if all its poles lie in the left half of the s-plane. Consequently, if the conversion technique is to be effective, it should possess the following desirable properties:

1. The $j\Omega$ axis in the s-plane should map into the unit circle in the z-plane. Thus there will be a direct relationship between the two frequency variables in the two domains.

2. The left-half plane (LHP) of the s-plane should map into the inside of the unit circle in the z-plane. Thus a stable analog filter will be converted to a stable digital filter.

We mentioned in the preceding section that physically realizable and stable IIR filters cannot have linear phase. Recall that a linear-phase filter must have a system function that satisfies the condition

$$H(z) = \pm z^{-N} H(z^{-1}) \tag{8.3.4}$$

where z^{-N} represents a delay of N units of time. But if this were the case, the filter would have a mirror-image pole outside the unit circle for every pole inside the unit circle. Hence the filter would be unstable. Consequently, a causal and stable IIR filter cannot have linear phase.

If the restriction on physical realizability is removed, it is possible to obtain a linear-phase IIR filter, at least in principle. This approach involves performing a time reversal of the input signal $x(n)$, passing $x(-n)$ through a digital filter $H(z)$, time-reversing the output of $H(z)$, and finally, passing the result through $H(z)$ again. This signal processing is computationally cumbersome and appears to offer no advantages over linear-phase FIR filters. Consequently, when an application requires a linear-phase filter, it should be an FIR filter.

In the design of IIR filters, we shall specify the desired filter characteristics for the magnitude response only. This does not mean that we consider the phase response unimportant. Since the magnitude and phase characteristics are related, as indicated in Section 8.1, we specify the desired magnitude characteristics and accept the phase response that is obtained from the design methodology.

8.3.1 IIR Filter Design by Approximation of Derivatives

One of the simplest methods for converting an analog filter into a digital filter is to approximate the differential equation in (8.3.3) by an equivalent difference equation. This approach is often used to solve a linear constant-coefficient differential equation numerically on a digital computer.

For the derivative $dy(t)/dt$ at time $t = nT$, we substitute the *backward difference* $[y(nT) - y(nT-1)]/T$. Thus

$$\begin{aligned}\left.\frac{dy(t)}{dt}\right|_{t=nT} &= \frac{y(nT) - y(nT-T)}{T} \\ &= \frac{y(n) - y(n-1)}{T}\end{aligned} \tag{8.3.5}$$

where T represents the sampling interval and $y(n) \equiv y(nT)$. The analog differentiator with output $dy(t)/dt$ has the system function $H(s) = s$, while the digital system that produces the output $[y(n) - y(n-1)]/T$ has the system function $H(z) = (1 - z^{-1})/T$. Consequently, as shown in Fig. 8.29, the frequency-domain

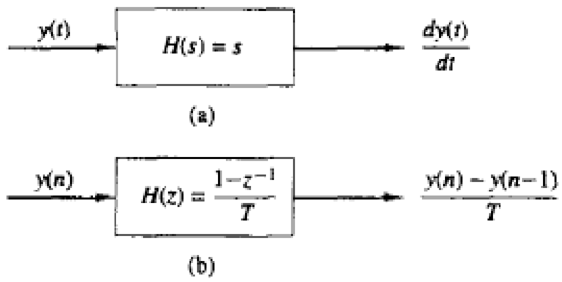

Figure 8.29 Substitution of the backward difference for the derivative implies the mapping $s = (1 - z^{-1})/T$.

equivalent for the relationship in (8.3.5) is

$$s = \frac{1 - z^{-1}}{T} \tag{8.3.6}$$

The second derivative $d^2y(t)/dt^2$ is replaced by the second difference, which is derived as follows:

$$\begin{aligned} \left.\frac{d^2y(t)}{dt^2}\right|_{t=nT} &= \frac{d}{dt}\left[\frac{dy(t)}{dt}\right]_{t=nT} \\ &= \frac{[y(nT) - y(nT - T)]/T - [y(nT - T) - y(nT - 2T)]/T}{T} \\ &= \frac{y(n) - 2y(n-1) + y(n-2)}{T^2} \end{aligned} \tag{8.3.7}$$

In the frequency domain, (8.3.7) is equivalent to

$$s^2 = \frac{1 - 2z^{-1} + z^{-2}}{T^2} = \left(\frac{1 - z^{-1}}{T}\right)^2 \tag{8.3.8}$$

It easily follows from the discussion that the substitution for the kth derivative of $y(t)$ results in the equivalent frequency-domain relationship

$$s^k = \left(\frac{1 - z^{-1}}{T}\right)^k \tag{8.3.9}$$

Consequently, the system function for the digital IIR filter obtained as a result of the approximation of the derivatives by finite differences is

$$H(z) = H_a(s)|_{s=(1-z^{-1})/T} \tag{8.3.10}$$

where $H_a(s)$ is the system function of the analog filter characterized by the differential equation given in (8.3.3).

Let us investigate the implications of the mapping from the s-plane to the z-plane as given by (8.3.6) or, equivalently,

$$z = \frac{1}{1 - sT} \tag{8.3.11}$$

If we substitute $s = j\Omega$ in (8.2.11), we find that

$$z = \frac{1}{1 - j\Omega T}$$

$$= \frac{1}{1+\Omega^2 T^2} + j\frac{\Omega T}{1+\Omega^2 T^2} \tag{8.3.12}$$

As Ω varies from $-\infty$ to ∞, the corresponding locus of points in the z-plane is a circle of radius $\frac{1}{2}$ and with center at $z = \frac{1}{2}$, as illustrated in Fig. 8.30.

It is easily demonstrated that the mapping in (8.3.11) takes points in the LHP of the s-plane into corresponding points inside this circle in the z-plane and points in the RHP of the s-plane are mapped into points outside this circle. Consequently, this mapping has the desirable property that a stable analog filter is transformed into a stable digital filter. However, the possible location of the poles of the digital filter are confined to relatively small frequencies and, as a consequence, the mapping is restricted to the design of lowpass filters and bandpass filters having relatively small resonant frequencies. It is not possible, for example, to transform a highpass analog filter into a corresponding highpass digital filter.

In an attempt to overcome the limitations in the mapping given above, more complex substitutions for the derivatives have been proposed. In particular, an Lth-order difference of the form

$$\left.\frac{dy(t)}{dt}\right|_{t=nT} = \frac{1}{T}\sum_{k=1}^{L}\alpha_k \frac{y(nT+kT) - y(nT-kT)}{T} \tag{8.3.13}$$

has been proposed, where $\{\alpha_k\}$ are a set of parameters that can be selected to optimize the approximation. The resulting mapping between the s-plane and the z-plane is now

$$s = \frac{1}{T}\sum_{k=1}^{L}\alpha_k(z^k - z^{-k}) \tag{8.3.14}$$

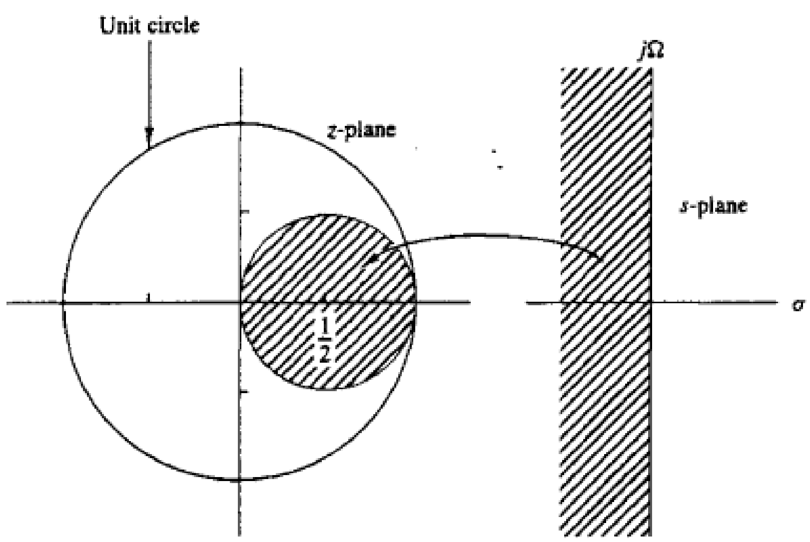

Figure 8.30 The mapping $s = (1 - z^{-1})/T$ takes LHP in the s-plane into points inside the circle of radius $\frac{1}{2}$ and center $z = \frac{1}{2}$ in the z-plane.

When $z = e^{j\omega}$, we have

$$s = j\frac{2}{T}\sum_{k=1}^{L}\alpha_k \sin \omega k \tag{8.3.15}$$

which is purely imaginary. Thus

$$\Omega = \frac{2}{T}\sum_{k=1}^{L}\alpha_k \sin \omega k \tag{8.3.16}$$

is the resulting mapping between the two frequency variables. By proper choice of the coefficients $\{\alpha_k\}$ it is possible to map the $j\Omega$-axis into the unit circle. Furthermore, points in the LHP in s can be mapped into points inside the unit circle in z.

Despite achieving the two desirable characteristics with the mapping of (8.3.16), the problem of selecting the set of coefficients $\{\alpha_k\}$ remains. In general, this is a difficult problem. Since simpler techniques exist for converting analog filters into IIR digital filters, we shall not emphasize the use of the Lth-order difference as a substitute for the derivative.

8.3.2 IIR Filter Design by Impulse Invariance

In the impulse invariance method, our objective is to design an IIR filter having a unit sample response $h(n)$ that is the sampled version of the impulse response of the analog filter. That is,

$$h(n) \equiv h(nT) \qquad n = 0, 1, 2, \dots \tag{8.3.17}$$

where T is the sampling interval.

To examine the implications of (8.3.17), we refer back to Section 4.2.9. Recall that when a continuous time signal $x_a(t)$ with spectrum $X_a(F)$ is sampled at a rate $F_s = 1/T$ samples per second, the spectrum of the sampled signal is the periodic repetition of the scaled spectrum $F_s X_a(F)$ with period F_s. Specifically, the relationship is

$$X(f) = F_s \sum_{k=-\infty}^{\infty} X_a[(f-k)F_s] \tag{8.3.18}$$

where $f = F/F_s$ is the normalized frequency. Aliasing occurs if the sampling rate F_s is less than twice the highest frequency contained in $X_a(F)$.

Expressed in the context of sampling the impulse response of an analog filter with frequency response $H_a(F)$, the digital filter with unit sample response $h(n) \equiv h_a(nT)$ has the frequency response

$$H(f) = F_s \sum_{k=-\infty}^{\infty} H_a[(f-k)F_s] \tag{8.3.19}$$

or, equivalently,

$$H(\omega) = F_s \sum_{k=-\infty}^{\infty} H_a[(\omega-2\pi k)F_s] \tag{8.3.20}$$

or

$$H(\Omega T) = \frac{1}{T} \sum_{k=-\infty}^{\infty} H_a \left(\Omega - \frac{2\pi k}{T} \right) \tag{8.3.21}$$

Figure 8.31 depicts the frequency response of a lowpass analog filter and the frequency response of the corresponding digital filter.

It is clear that the digital filter with frequency response $H(\omega)$ has the frequency response characteristics of the corresponding analog filter if the sampling interval T is selected sufficiently small to completely avoid or at least minimize the effects of aliasing. It is also clear that the impulse invariance method is inappropriate for designing highpass filters due the to spectrum aliasing that results from the sampling process.

To investigate the mapping of points between the z-plane and the s-plane implied by the sampling process, we rely on a generalization of (8.3.21) which relates the z-transform of $h(n)$ to the Laplace transform of $h_a(t)$. This relationship is

$$H(z)|_{z=e^{sT}} = \frac{1}{T} \sum_{k=-\infty}^{\infty} H_a \left(s - j\frac{2\pi k}{T} \right) \tag{8.3.22}$$

where

$$H(z) = \sum_{n=0}^{\infty} h(n) z^{-n}$$

$$H(z)|_{z=e^{sT}} = \sum_{n=0}^{\infty} h(n) e^{-sTn} \tag{8.3.23}$$

Note that when $s = j\Omega$, (8.3.22) reduces to (8.3.21), where the factor of j in $H_a(\Omega)$ is suppressed in our notation.

Let us consider the mapping of points from the s-plane to the z-plane implied by the relation

$$z = e^{sT} \tag{8.3.24}$$

If we substitute $s = \sigma + j\Omega$ and express the complex variable z in polar form as $z = re^{j\omega}$, (8.3.24) becomes

$$re^{j\omega} = e^{\sigma T} e^{j\Omega T}$$

Clearly, we must have

$$\begin{aligned} r &= e^{\sigma T} \\ \omega &= \Omega T \end{aligned} \tag{8.3.25}$$

Consequently, $\sigma < 0$ implies that $0 < r < 1$ and $\sigma > 0$ implies that $r > 1$. When $\sigma = 0$, we have $r = 1$. Therefore, the LHP in s is mapped inside the unit circle in z and the RHP in s is mapped outside the unit circle in z.

Also, the $j\Omega$-axis is mapped into the unit circle in z as indicated above. However, the mapping of the $j\Omega$-axis into the unit circle is not one-to-one. Since ω is unique over the range $(-\pi, \pi)$, the mapping $\omega = \Omega T$ implies that the interval $-\pi/T \le \Omega \le \pi/T$ maps into the corresponding values of $-\pi \le \omega \le \pi$. Furthermore, the frequency interval $\pi/T \le \Omega \le 3\pi/T$ also maps into the interval $-\pi \le \omega \le \pi$ and, in general, so does the interval $(2k-1)\pi/T \le \Omega \le (2k+1)\pi/T$, when k is an integer. Thus the mapping from the analog frequency Ω to the frequency variable ω in the digital domain is many-to-one, which simply reflects the effects of aliasing due to sampling. Figure 8.32 illustrates the mapping from the s-plane to the z-plane for the relation in (8.3.24).

To explore further the effect of the impulse invariance design method on the characteristics of the resulting filter, let us express the system function of the analog filter in partial-fraction form. On the assumption that the poles of the analog filter are distinct, we can write

$$H_a(s) = \sum_{k=1}^{N} \frac{c_k}{s - p_k} \tag{8.3.26}$$

where $\{p_k\}$ are the poles of the analog filter and $\{c_k\}$ are the coefficients in the partial-fraction expansion. Consequently,

$$h_a(t) = \sum_{k=1}^{N} c_k e^{p_k t} \qquad t \ge 0 \tag{8.3.27}$$

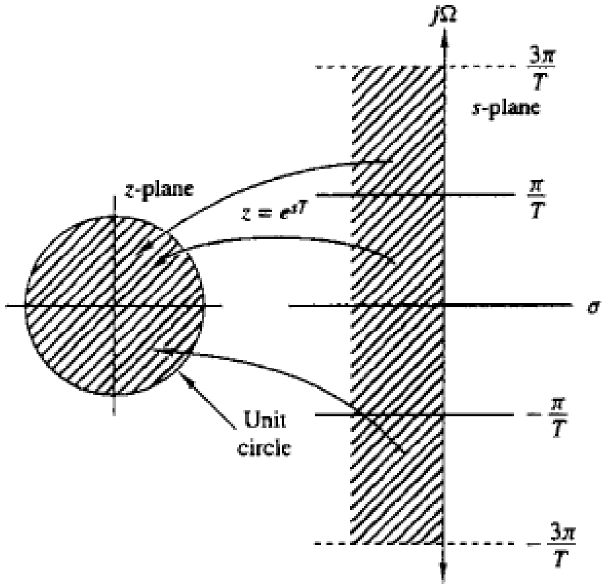

Figure 8.32 The mapping of $z = e^{sT}$ maps strips of width $2\pi/T$ (for $\sigma < 0$) in the s-plane into points in the unit circle in the z-plane.

If we sample $h_a(t)$ periodically at $t = nT$, we have

$$\begin{aligned} h(n) &= h_a(nT) \\ &= \sum_{k=1}^{N} c_k e^{p_k T n} \end{aligned} \tag{8.3.28}$$

Now, with the substitution of (8.3.28), the system function of the resulting digital IIR filter becomes

$$\begin{aligned} H(z) &= \sum_{n=0}^{\infty} h(n) z^{-n} \\ &= \sum_{n=0}^{\infty} \left(\sum_{k=1}^{N} c_k e^{p_k T n} \right) z^{-n} \\ &= \sum_{k=1}^{N} c_k \sum_{n=0}^{\infty} (e^{p_k T} z^{-1})^n \end{aligned} \tag{8.3.29}$$

The inner sum in (8.3.29) converges because $p_k < 0$ and yields

$$\sum_{n=0}^{\infty} (e^{p_k T} z^{-1})^n = \frac{1}{1 - e^{p_k T} z^{-1}} \tag{8.3.30}$$

Therefore, the system function of the digital filter is

$$H(z) = \sum_{k=1}^{N} \frac{c_k}{1 - e^{p_k T} z^{-1}} \tag{8.3.31}$$

We observe that the digital filter has poles at

$$z_k = e^{p_k T} \qquad k = 1, 2, \ldots, N \tag{8.3.32}$$

8.3.3 IIR Filter Design by the Bilinear Transformation

The IIR filter design techniques described in the preceding two sections have a severe limitation in that they are appropriate only for lowpass filters and a limited class of bandpass filters.

In this section we describe a mapping from the s-plane to the z-plane, called the bilinear transformation, that overcomes the limitation of the other two design methods described previously. The bilinear transformation is a conformal mapping that transforms the $j\Omega$-axis into the unit circle in the z-plane only once, thus avoiding aliasing of frequency components. Furthermore, all points in the LHP of s are mapped inside the unit circle in the z-plane and all points in the RHP of s are mapped into corresponding points outside the unit circle in the z-plane.

The bilinear transformation can be linked to the trapezoidal formula for numerical integration. For example, let us consider an analog linear filter with system function

$$H(s) = \frac{b}{s+a} \tag{8.3.33}$$

This system is also characterized by the differential equation

$$\frac{dy(t)}{dt} + ay(t) = bx(t) \tag{8.3.34}$$

Instead of substituting a finite difference for the derivative, suppose that we integrate the derivative and approximate the integral by the trapezoidal formula. Thus

$$y(t) = \int_{t_0}^{t} y'(\tau)d\tau + y(t_0) \tag{8.3.35}$$

where $y'(t)$ denotes the derivative of $y(t)$. The approximation of the integral in (8.3.35) by the trapezoidal formula at $t = nT$ and $t_0 = nT - T$ yields

$$y(nT) = \frac{T}{2}[y'(nT) + y'(nT - T)] + y(nT - T) \tag{8.3.36}$$

Now the differential equation in (8.3.34) evaluated at $t = nT$ yields

$$y'(nT) = -ay(nT) + bx(nT) \tag{8.3.37}$$

We use (8.3.37) to substitute for the derivative in (8.3.36) and thus obtain a difference equation for the equivalent discrete-time system. With $y(n) \equiv y(nT)$ and $x(n) \equiv x(nT)$, we obtain the result

$$\left(1 + \frac{aT}{2}\right) y(n) - \left(1 - \frac{aT}{2}\right) y(n-1) = \frac{bT}{2}[x(n) + x(n-1)] \tag{8.3.38}$$

The z-transform of this difference equation is

$$\left(1 + \frac{aT}{2}\right) Y(z) - \left(1 - \frac{aT}{2}\right) z^{-1} Y(z) = \frac{bT}{2}(1 + z^{-1})X(z)$$

Consequently, the system function of the equivalent digital filter is

$$H(z) = \frac{Y(z)}{X(z)} = \frac{(bT/2)(1 + z^{-1})}{1 + aT/2 - (1 - aT/2)z^{-1}}$$

or, equivalently,

$$H(z) = \frac{b}{\dfrac{2}{T}\left(\dfrac{1 - z^{-1}}{1 + z^{-1}}\right) + a} \tag{8.3.39}$$

Clearly, the mapping from the s-plane to the z-plane is

$$s = \frac{2}{T}\left(\frac{1-z^{-1}}{1+z^{-1}}\right) \tag{8.3.40}$$

This is called the *bilinear transformation.*

Although our derivation of the bilinear transformation was performed for a first-order differential equation, it holds, in general, for an Nth-order differential equation.

To investigate the characteristics of the bilinear transformation, let

$$z = re^{j\omega}$$

$$s = \sigma + j\Omega$$

Then (8.3.40) can be expressed as

$$\begin{aligned} s &= \frac{2}{T}\frac{z-1}{z+1} \\ &= \frac{2}{T}\frac{re^{j\omega}-1}{re^{j\omega}+1} \\ &= \frac{2}{T}\left(\frac{r^2-1}{1+r^2+2r\cos\omega} + j\frac{2r\sin\omega}{1+r^2+2r\cos\omega}\right) \end{aligned}$$

Consequently,

$$\sigma = \frac{2}{T}\frac{r^2-1}{1+r^2+2r\cos\omega} \tag{8.3.41}$$

$$\Omega = \frac{2}{T}\frac{2r\sin\omega}{1+r^2+2r\cos\omega} \tag{8.3.42}$$

First, we note that if $r < 1$, then $\sigma < 0$, and if $r > 1$, then $\sigma > 0$. Consequently, the LHP in s maps into the inside of the unit circle in the z-plane and the RHP in s maps into the outside of the unit circle. When $r = 1$, then $\sigma = 0$ and

$$\begin{aligned} \Omega &= \frac{2}{T}\frac{\sin\omega}{1+\cos\omega} \\ &= \frac{2}{T}\tan\frac{\omega}{2} \end{aligned} \tag{8.3.43}$$

or, equivalently,

$$\omega = 2\tan^{-1}\frac{\Omega T}{2} \tag{8.3.44}$$

The relationship in (8.3.44) between the frequency variables in the two domains is illustrated in Fig. 8.36. We observe that the entire range in Ω is mapped only once into the range $-\pi \le \omega \le \pi$. However, the mapping is highly nonlinear. We observe a frequency compression or *frequency warping*, as it is usually called, due to the nonlinearity of the arctangent function.

It is also interesting to note that the bilinear transformation maps the point $s = \infty$ into the point $z = -1$. Consequently, the single-pole lowpass filter in

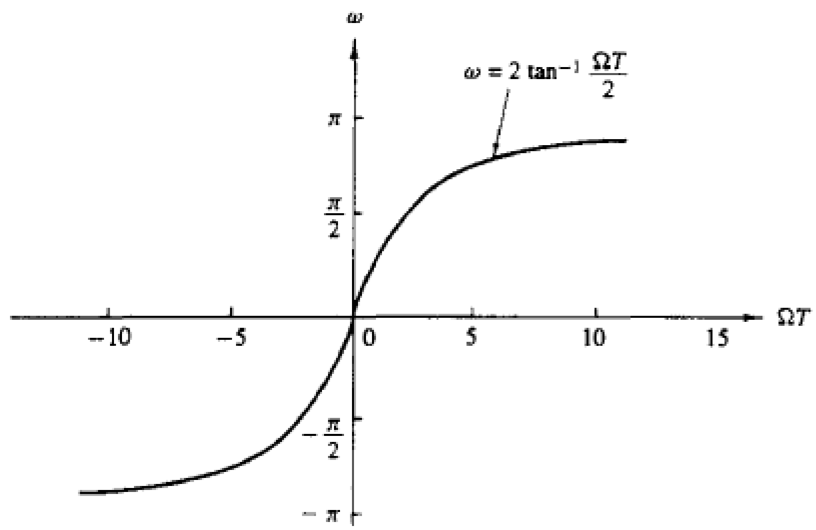

Chebyshev filters. There are two types of Chebyshev filters. Type I Chebyshev filters are all-pole filters that exhibit equiripple behavior in the passband and a monotonic characteristic in the stopband. On the other hand, the family of type II Chebyshev filters contains both poles and zeros and exhibits a monotonic behavior in the passband and an equiripple behavior in the stopband. The zeros of this class of filters lie on the imaginary axis in the s-plane.

The magnitude squared of the frequency response characteristic of a type I Chebyshev filter is given as

$$|H(\Omega)|^2 = \frac{1}{1+\epsilon^2 T_N^2(\Omega/\Omega_p)} \tag{8.3.51}$$

where ϵ is a parameter of the filter related to the ripple in the passband and $T_N(x)$ is the Nth-order Chebyshev polynomial defined as

$$T_N(x) = \begin{cases} \cos(N\cos^{-1}x), & |x| \le 1 \\ \cosh(N\cosh^{-1}x), & |x| > 1 \end{cases} \tag{8.3.52}$$

The Chebyshev polynomials can be generated by the recursive equation

$$T_{N+1}(x) = 2xT_N(x) - T_{N-1}(x) \qquad N = 1, 2, \ldots \tag{8.3.53}$$

where $T_0(x) = 1$ and $T_1(x) = x$. From (8.3.53) we obtain $T_2(x) = 2x^2 - 1$, $T_3(x) = 4x^3 - 3x$, and so on.

Some of the properties of these polynomials are as follows:

1. $|T_N(x)| \le 1$ for all $|x| \le 1$.
2. $T_N(1) = 1$ for all N.
3. All the roots of the polynomial $T_N(x)$ occur in the interval $-1 \le x \le 1$.

The filter parameter ϵ is related to the ripple in the passband, as illustrated in Fig. 8.39, for N odd and N even. For N odd, $T_N(0) = 0$ and hence $|H(0)|^2 = 1$. On the other hand, for N even, $T_N(0) = 1$ and hence $|H(0)|^2 = 1/(1 + \epsilon^2)$. At the band edge frequency $\Omega = \Omega_p$, we have $T_N(1) = 1$, so that

$$\frac{1}{\sqrt{1+\epsilon^2}} = 1 - \delta_1$$

or, equivalently,

$$\epsilon^2 = \frac{1}{(1-\delta_1)^2} - 1 \tag{8.3.54}$$

where δ_1 is the value of the passband ripple.

The poles of a type I Chebyshev filter lie on an ellipse in the s-plane with major axis

$$r_1 = \Omega_p \frac{\beta^2 + 1}{2\beta} \tag{8.3.55}$$

and minor axis

$$r_2 = \Omega_p \frac{\beta^2 - 1}{2\beta} \tag{8.3.56}$$

where β is related to ϵ according to the equation

$$\beta = \left[\frac{\sqrt{1+\epsilon^2} + 1}{\epsilon} \right]^{1/N} \tag{8.3.57}$$

The pole locations are most easily determined for a filter of order N by first locating the poles for an equivalent Nth-order Butterworth filter that lie on circles of radius r_1 or radius r_2, as illustrated in Fig. 8.40. If we denote the angular positions of the poles of the Butterworth filter as

$$\phi_k = \frac{\pi}{2} + \frac{(2k+1)\pi}{2N} \qquad k = 0, 1, 2, \ldots, N-1 \tag{8.3.58}$$

then the positions of the poles for the Chebyshev filter lie on the ellipse at the coordinates (x_k, y_k), $k = 0, 1, \ldots, N-1$, where

$$\begin{aligned} x_k &= r_2 \cos\phi_k, \qquad k = 0, 1, \ldots, N-1 \\ y_k &= r_1 \sin\phi_k, \qquad k = 0, 1, \ldots, N-1 \end{aligned} \tag{8.3.59}$$

A type II Chebyshev filter contains zeros as well as poles. The magnitude squared of its frequency response is given as

$$|H(\Omega)|^2 = \frac{1}{1 + \epsilon^2[T_N^2(\Omega_s/\Omega_p)/T_N^2(\Omega_s/\Omega)]} \tag{8.3.60}$$

where $T_N(x)$ is, again, the Nth-order Chebyshev polynomial and Ω_s is the stopband frequency as illustrated in Fig. 8.41. The zeros are located on the imaginary axis at the points

$$s_k = j\frac{\Omega_s}{\sin\phi_k} \qquad k = 0, 1, \ldots, N-1 \tag{8.3.61}$$

The poles are located at the points (v_k, w_k), where

$$v_k = \frac{\Omega_s x_k}{\sqrt{x_k^2 + y_k^2}} \qquad k = 0, 1, \ldots, N-1 \tag{8.3.62}$$

$$w_k = \frac{\Omega_s y_k}{\sqrt{x_k^2 + y_k^2}} \qquad k = 0, 1, \ldots, N-1 \tag{8.3.63}$$

where $\{x_k\}$ and $\{y_k\}$ are defined in (8.3.59) with β now related to the ripple in the stopband through the equation

$$\beta = \left[\frac{1 + \sqrt{1 - \delta_2^2}}{\delta_2}\right]^{1/N} \tag{8.3.64}$$

$$N = \frac{\log\left[\left(\sqrt{1-\delta_2^2} + \sqrt{1-\delta_2^2(1+\epsilon^2)}\right)/\epsilon\delta_2\right]}{\log\left[(\Omega_s/\Omega_p) + \sqrt{(\Omega_s/\Omega_p)^2 - 1}\right]}$$

$$= \frac{\cosh^{-1}(\delta/\epsilon)}{\cosh^{-1}(\Omega_s/\Omega_p)}$$

where, by definition, $\delta_2 = 1/\sqrt{1+\delta^2}$.

Frequency Transformations in the Analog Domain

Type of transformation	Transformation	Band edge frequencies of new filter
Lowpass	$s \longrightarrow \frac{\Omega_p}{\Omega'_p} s$	Ω'_p
Highpass	$s \longrightarrow \frac{\Omega_p \Omega'_p}{s}$	Ω'_p
Bandpass	$s \longrightarrow \Omega_p \frac{s^2 + \Omega_l \Omega_u}{s(\Omega_u - \Omega_l)}$	Ω_l, Ω_u
Bandstop	$s \longrightarrow \Omega_p \frac{s(\Omega_u - \Omega_c)}{s^2 + \Omega_u \Omega_l}$	Ω_l, Ω_u

Frequency Transformations in the Digital Domain

Type of transformation	Transformation	Parameters
Lowpass	$z^{-1} \longrightarrow \dfrac{z^{-1} - a}{1 - az^{-1}}$	ω'_p = band edge frequency of new filter $a = \dfrac{\sin[(\omega_p - \omega'_p)/2]}{\sin[(\omega_p + \omega'_p)/2]}$
Highpass	$z^{-1} \longrightarrow -\dfrac{z^{-1} + a}{1 + az^{-1}}$	ω'_p = band edge frequency new filter $a = -\dfrac{\cos[(\omega_p + \omega'_p)/2]}{\cos[(\omega_p - \omega'_p)/2]}$
Bandpass	$z^{-1} \longrightarrow -\dfrac{z^{-2} - a_1 z^{-1} + a_2}{a_2 z^{-2} - a_1 z^{-1} + 1}$	ω_l = lower band edge frequency ω_u = upper band edge frequency $a_1 = -2\alpha K/(K+1)$ $a_2 = (K-1)/(K+1)$ $\alpha = \dfrac{\cos[(\omega_u + \omega_l)/2]}{\cos[(\omega_u - \omega_l)/2]}$ $K = \cot \dfrac{\omega_u - \omega_l}{2} \tan \dfrac{\omega_p}{2}$
Bandstop	$z^{-1} \longrightarrow -\dfrac{z^{-2} - a_1 z^{-1} + a_2}{a_2 z^{-2} - a_1 z^{-1} + 1}$	ω_l = lower band edge frequency ω_u = upper band edge frequency $a_1 = -2\alpha/(K+1)$ $a_2 = (1-K)/(1+K)$ $\alpha = \dfrac{\cos[(\omega_u + \omega_l)/2]}{\cos[(\omega_u - \omega_l)/2]}$ $K = \tan \dfrac{\omega_u - \omega_l}{2} \tan \dfrac{\omega_p}{2}$

****